Clustering due to Acceleration in the Response to Population Gradient: A Simple Self-Organization Model

Yuri Tyutyunov,[1,*] Inna Senina,[1,†] and Roger Arditi[2,‡]

1. Laboratory of Mathematical Modelling of Biological Processes, Department of Mathematical Modelling in Ecology and Economics, Vorovich Research Institute of Mechanics and Applied Mathematics, Rostov State University, Stachki Street 200/1, 344090 Rostov-on-Don, Russia;
2. Écologie des Populations et Communautés, Institut National Agronomique Paris-Grignon, 16 rue Claude Bernard, 75231 Paris Cedex 05, France

ABSTRACT: We explore the phenomenon of animal self-organization due to autotaxis, that is, the movement of individuals induced by their own density gradient. There is natural evidence that clustering occurs as a result of the interplay between random and directed movements of individuals due to mutual attraction and repulsion. Classically, it is assumed that taxis velocity is determined by the density gradient of some stimulus. However, it is known that partial differential equation (PDE) diffusion-advection models that rest on this assumption cannot give a realistic representation of a stationary or moving cohesive group of individuals with a uniform interior density and sharp edges. Pioneering work by Okubo and coworkers suggests that the acceleration of individuals (rather than their velocity directly) is proportional to the population density gradient. A PDE model resting on this finding was constructed and investigated. The model demonstrates the formation of steady heterogeneous structures of the required shape. This feature can be interpreted as dynamic self-organization, like fish shoaling or insect swarming. This model is the first to achieve this result while considering an autonomous population in a simple PDE framework. Analytical and numerical studies show that the link between the acceleration and the density gradient is crucial for the appearance of clusters.

* E-mail: ytyutyun@math.rsu.ru.

† Present address: Joint Institute for Marine and Atmospheric Research, Pelagic Fisheries Research Program, University of Hawaii at Manoa, Honolulu, Hawaii 96822; e-mail: senina@hawaii.edu.

‡ E-mail: arditi@inapg.fr.

Keywords: taxis-diffusion partial differential equation, nonuniform steady state, animal aggregation, swarming.

The formation of spatial aggregates of animals, that is, clustering, is a common phenomenon inherent to a variety of biological species, from microscopic colonies of bacteria, swarms of larvae, or adult insects to macroscopic fish schools, bird flocks, and others (Keller and Segel 1970; Prigogine and Stengers 1984; Deneubourg et al. 1990; Parrish et al. 2002; Jeanson et al. 2003, 2004). The fundamental mechanism of self-organization is individual taxis, which is commonly due to the spatial heterogeneity of environmental or internal population factors. Although in reality more than one mechanism may underlie animal aggregation (Grünbaum and Okubo 1994), we will focus in this work on the case in which the taxis stimulus leading to spatial grouping is the heterogeneity of the density of conspecifics only, within a uniform environment. Hereafter, we will call this self-organization mechanism autotaxis. Such an intrinsic mode of clustering, characterized by the mutual attraction and repulsion of individuals, is common among animals, examples being swarming locusts (Edelstein-Keshet et al. 1998), midges (Okubo et al. 1977), and schooling fish (Parrish and Turchin 1997; Parrish et al. 2002).

Observed biological features of the aggregation mechanism can lead to the basic assumptions of a mathematical model of clustering and set requirements on its properties. A common observation is that clustering occurs because of the behavioral interplay between random and directional movements of individuals (Prigogine and Stengers 1984; Deneubourg et al. 1990). For example, studying the movements of swarming midges, Okubo et al. (1977) identified that the presence of an attractive "force" toward the center of the swarm plays a crucial role in maintaining the cluster against the general tendency to disperse because of random motion. Together with mutual attraction, the other directional force that should be taken into account is repulsion, which occurs when the density becomes too high.

The model must demonstrate the formation of one or

several groups of individuals with realistic cluster profiles, characterized by a constant interior density and a high-density gradient at the edges (Grünbaum 1994; Mogilner and Edelstein-Keshet 1999). The uniform density in the cluster interior results from the opposed forces of attraction and repulsion and is manifested in an almost constant distance between individuals. Each species has a certain critical distance (i.e., a critical density) that determines a switch between the dominance of attraction or repulsion (Breder 1959; Camazine et al. 2003). For example, the mean distance to the nearest neighbor varies among fish species between 0.3 and 3 body lengths (Adioui et al. 2003).

Commonly, mathematical models of spatial dynamics of animals follow either the Lagrangian or the Eulerian approaches. Lagrangian models describe the characteristics of individuals and apply Newtonian mechanics to the velocity and acceleration of moving organisms (Grünbaum and Okubo 1994; Turchin 1998; Flierl et al. 1999). Eulerian models follow the spatiotemporal dynamics of population density, for example, with systems of partial differential equations (PDE; Okubo 1980; Murray 1993; Okubo and Levin 2001). Both approaches conventionally assume that the interactions among the members and with the environment are represented by gradient forces (Niwa 1996; Mogilner and Edelstein-Keshet 2003). In Eulerian models, the reaction of animals to these forces is taken into account as density-dependent diffusion and advection terms (Keller and Segel 1970; Mimura and Kawasaki 1980; Okubo 1980; Seno and Nakai 1995; Czárán 1998). An important problem is that of linking the microscopic and macroscopic properties of behavior in both approaches. The development of techniques for translating from Lagrangian to Eulerian models, with an explicit correspondence between density-dependent individual behavior and flux reaction terms, is the subject of active research (Grünbaum 1994, 2002; Grünbaum and Okubo 1994; Flierl et al. 1999; Cantrell and Cosner 2004).

As recognized only recently (Edelstein-Keshet et al. 1998; Mogilner and Edelstein-Keshet 1999), conventional mathematical models of spatiotemporal population dynamics based on PDE systems with advective (tactic) and diffusive terms fail to provide a realistic representation of the formation and movement of a finite group of individuals like a swarm or flock in a homogeneous and steady environment. Therefore, taxis must be described differently in continuous models. As a possible solution to this theoretical problem, Mogilner and Edelstein-Keshet (1999) constructed a model for a moving cohesive swarm using partial integro-differential equations. In their model, the advective velocity of the individuals is assumed to be influenced by nonlocal interactions; attractive and repulsive terms at each point are determined by the density distribution over some area (Mogilner and Edelstein-Keshet 1999). The main result is that "if density dependence in the repulsion term is of a higher order than in the attraction term, then the swarm profile is realistic; that is, the swarm has a constant interior density with sharp edges, as observed in biological examples" (Mogilner and Edelstein-Keshet 1999, p. 534). Earlier, Grünbaum (1994) had also proposed a partial integro-differential equation producing a realistic profile of a stationary animal aggregation within a closed domain. This nonlocal model was derived from a Lagrangian algorithm for social behavior of swarming individuals seeking the preferred population density.

In this work, we present an alternative, novel approach that rests only on local information, without reference to the global pattern. Fulfilling all requirements of model adequacy posed by Mogilner and Edelstein-Keshet (1999), the model is an autonomous taxis-diffusion system of PDEs. It differs from conventional PDE models with taxis that assume the dependence of the velocity on the gradient of some stimulus (Keller and Segel 1970; Czárán 1998; Hillen and Painter 2001; Hillen and Potapov 2004; Tsyganov et al. 2003). Instead, we make the assumption that the taxis acceleration (rather than the velocity directly) is determined by the density gradient, an assumption that is commonly used in the Lagrangian framework of description of individual active behavior (Grünbaum and Okubo 1994; Turchin 1998). We use it in our Eulerian model in order to take into account the forces of attraction and repulsion. We will show that this mechanistic assumption is strongly supported by the kinematic analysis of a midge swarm performed by Okubo et al. (1977).

Mechanistic Description of Individual Motion within the PDE Model

In a pioneering experimental study, Okubo et al. (1977) analyzed the trajectory of swarming midges (*Anarete pritchardi* Kim), observing the trajectories, velocities, and accelerations of individuals. This study, which is unique in its level of detail, shows that our hypothesis about taxis acceleration agrees very well with the observations. Projecting the midge movements onto the horizontal plane, Okubo and coauthors showed that the acceleration of each insect at the center of the swarm is very close to 0 (fig. 1). At the edge of the swarm, accelerations toward the center are highest. In the center of the swarm, midges fly more or less randomly. A similar behavior was also detected in laboratory observations of juvenile blacksmith (*Chromis punctipinnis*; Parrish and Turchin 1997). The attraction of fish individuals toward the school center is always positive and gradually increases in strength with distance to the center. Although data were collected only
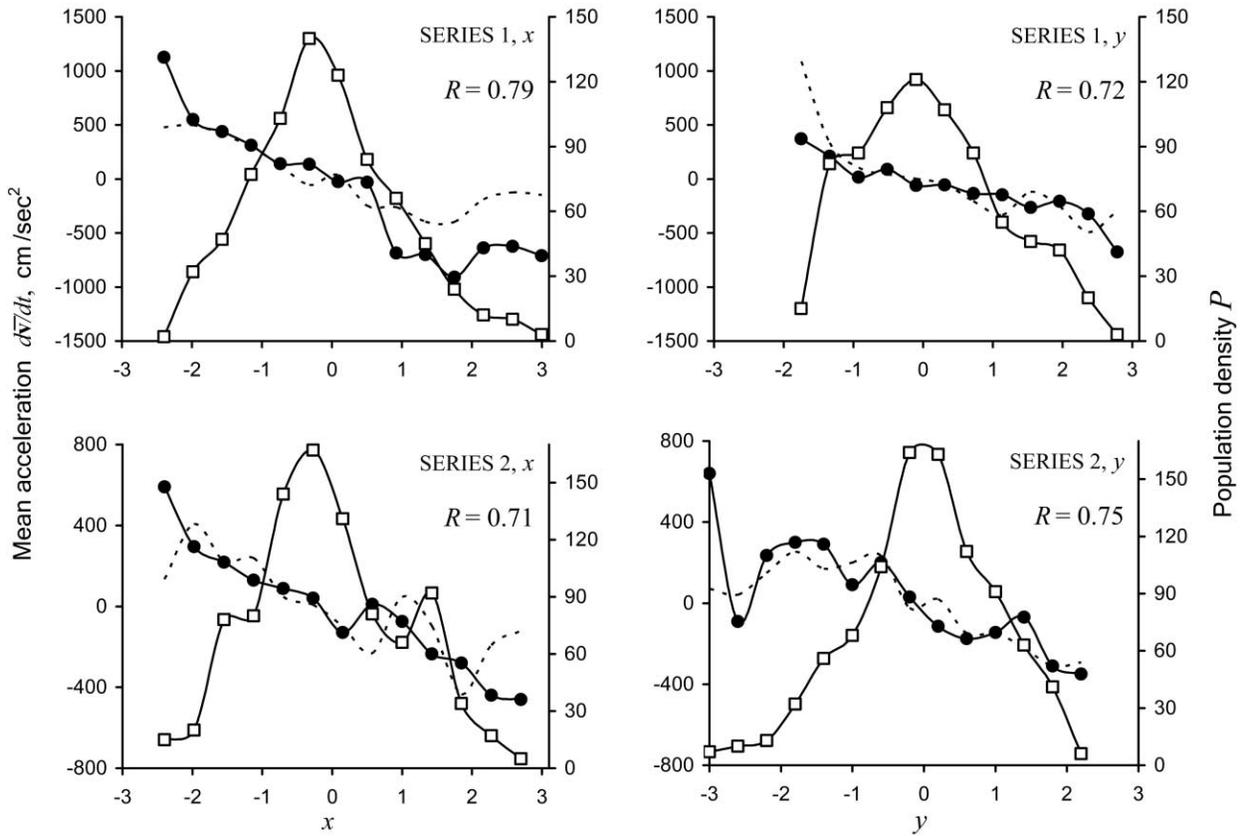
Figure 1: Mean values of acceleration $d\mathbf{v}/dt$ (*black circles*) and density of individuals (*open squares*) within a swarm of midges projected onto the horizontal plane (x, y); *Series 1* and *Series 2* refer to two experiments by Okubo et al. (1977). The normalized coordinates are centered at the swarm center of mass with one unit being 1 SD of midge positions. The left graphs are projections on the *X*-axis; those on the right are on the *Y*-axis. The dashed curves show the best fit of equation (1) to the observed values of midge accelerations. *R* is the multiple correlation coefficient.

within the congregation, it is clear that the attraction must be limited to some distance because individuals that are very far away cannot sense the group.

From Okubo et al.'s (1977) data, we notice that the center of the swarm is the place where the density of midges is highest and its gradient is 0. At the edge of the swarm, the density is lowest and its gradient is highest. Thus, the simplest relationship between acceleration and density gradient appears to be $d\mathbf{v}/dt = \kappa\nabla P$, where $\mathbf{v} = \mathbf{v}(\mathbf{x}, t)$ is the midges's velocity vector at point $\mathbf{x} = (x, y)$, $P = P(\mathbf{x}, t)$ is the population density, and κ is the autotaxis coefficient. Also, in order to include repulsion, we must add a term leading to a change of direction when the density reaches the critical value P_c, that is, when $P > P_c$, the force affecting the movement of animals, changes to repulsion down their own density gradient. The simplest way to express this is to change the taxis coefficient as $\kappa \rightarrow \kappa(1 - P/P_c)$, and we obtain

$$\frac{d\mathbf{v}}{dt} = \kappa\left(1 - \frac{P}{P_c}\right)\nabla P. \qquad (1)$$

Okubo et al.'s (1977) observations of density and acceleration distributions and the best fit of equation (1) to the accelerations are superimposed in figure 1. In order to fit equation (1) to the observed accelerations, we used central differences to approximate the gradient at each ith spatial position with the formula $\nabla P_i \approx (P_{i+1} - P_{i-1})/2h$, where h is the step of the spatial grid used by Okubo et al. (1977) and P_i represents the observed swarm densities. As shown by the graphs, the proposed expression for the acceleration fits very well to the natural observations, with adjustment of the two free parameters κ and P_c.

Thus, this article proposes a swarming model based on an autonomous system of advection-diffusion equations in which the acceleration of individuals is determined by their own density gradient according to the relationship

in equation (1). Without any other processes than directed and random movement of animals, we will analyze the conditions for breaking the stability of the homogeneous equilibrium, and we will show that stationary and dynamic spatially heterogeneous solutions emerge that can be interpreted as the formation of persistent groups of individuals. Our earlier work (Govorukhin et al. 1999, 2000; Arditi et al. 2001; Tyutyunov et al. 2002; Sapoukhina et al. 2003) has demonstrated that, in a predator-prey system, a similar assumption about the predator acceleration (proportional to the prey density gradient $d\mathbf{v}/dt = \kappa\nabla N$) leads to qualitatively appropriate spatiotemporal dynamics that cannot be obtained with the conventional assumption $\mathbf{v} = \kappa\nabla N$.

The Model

Equation (1) is the core of the model. Coupling it with a standard taxis-diffusion equation, we obtain the following PDE system for the spatiotemporal dynamics of the aggregating group of animals:

$$\frac{\partial P}{\partial t} + \text{div}(P\mathbf{v}) = \delta_p \Delta P, \tag{2}$$

$$\frac{\partial \mathbf{v}}{\partial t} = \kappa\left(1 - \frac{P}{P_c}\right)\nabla P + \delta_v \Delta \mathbf{v}, \tag{3}$$

where δ_p and δ_v are diffusion coefficients. Local variations of population density occur only because of diffusive and advective flows. The diffusive and advective terms in the balance equation (2) describe random and directed movements of the population density, respectively. Equation (3) is modified from equation (1) by the inclusion of a diffusion term for the velocity in order to represent the forces that equalize velocities of neighbors (Flierl et al. 1999). Since the value of coefficient δ_v, which is an analogue of mechanical viscosity, should be very small for moving fish or insect individuals, the fit done in the previous section on Okubo et al.'s (1977) data must remain valid. In the following mathematical analysis, we only require positiveness of δ_v, which can be arbitrarily small.

Boundary conditions are of great importance in the determination of the form of the solutions. They are specified in such a way that the boundary of the domain Ω is impenetrable:

$$\mathbf{n} \cdot \nabla P|_{\mathbf{x}\in\partial\Omega} = \mathbf{n} \cdot \mathbf{v}|_{\mathbf{x}\in\partial\Omega} = 0, \tag{4}$$

where $\partial\Omega$ is the boundary and $\mathbf{n}$ is the unit normal vector.

The model is entirely specified by equations (2)–(4). According to these equations, the average value of the density of the whole population does not vary with time:

$$\frac{1}{\text{Vol}(\Omega)}\int_\Omega P(\mathbf{x}, t)d\mathbf{x} = \overline{P} = \text{constant}.$$

Linear Analysis

We first investigate a two-dimensional (2-D) case of model (2)–(4), considering a closed rectangular domain Ω with lengths L_1, L_2. The model has the spatially homogeneous equilibrium:

$$P^*(\mathbf{x}, t) \equiv \overline{P}, \mathbf{v}^*(\mathbf{x}, t) \equiv 0. \tag{5}$$

The linear analysis (see Murray 1993 for the method) consists in the investigation of the stability of equilibrium (5) with respect to small spatially heterogeneous perturbations. For this purpose, we must linearize the equations (2), (3) in the vicinity of equilibrium (5) and look for nonzero solutions of the perturbed variables $p(\mathbf{x}, t) = P(\mathbf{x}, t) - \overline{P}$ and $\mathbf{v}(\mathbf{x}, t)$ in the form of a Fourier expansion:

$$p(x, y, t) = \sum_{m, n \geq 0} p_{mn}\cos\frac{\pi m}{L_1}x \cdot \cos\frac{\pi n}{L_2}y \cdot e^{\lambda_{mn}t},$$

$$[v_1(x, y, t), v_2(x, y, t)] =$$

$$\sum_{m, n \geq 0}\left(v_{1mn}\sin\frac{\pi m}{L_1}x \cdot \sin\frac{\pi n}{L_2}y,\right.$$

$$\left.v_{2mn}\sin\frac{\pi m}{L_1}x \cdot \sin\frac{\pi n}{L_2}y\right) \cdot e^{\lambda_{mn}t},$$

where p_{mn}, v_{1mn}, and v_{2mn} are constants, and "cos" and "sin" are used, respectively, for p and $\mathbf{v}$ in order to satisfy the boundary conditions (4). The eigenvalues λ_{mn} are the zeros of the characteristic polynomial

$$\chi(\lambda_{mn}) = (\lambda_{mn} + \delta_v k_{mn}^2)\chi_1(\lambda_{mn}), \tag{6a}$$

with

$$\chi_1(\lambda_{mn}) = \lambda_{mn}^2 + k_{mn}^2(\delta_v + \delta_p)\lambda_{mn}$$
$$+ \delta_v\delta_p k_{mn}^4 - \kappa\overline{P}(1 - \overline{P}/P_c)k_{mn}^2, \tag{6b}$$

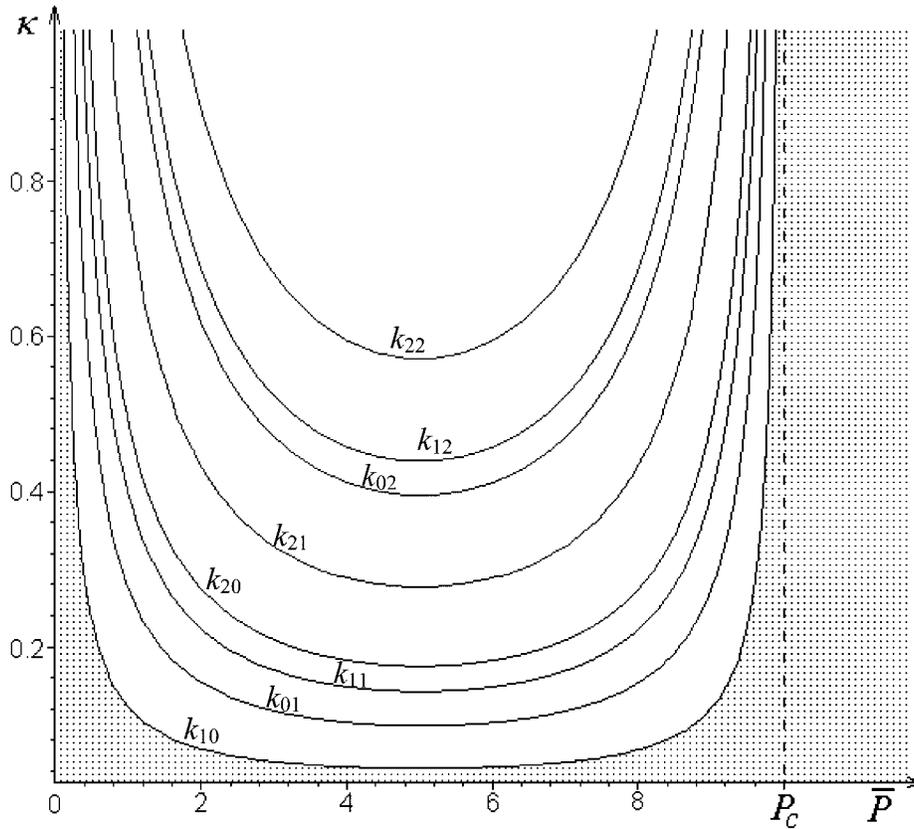where the so-called wave numbers, k_{mn}, are defined as

Figure 2: Critical stability curves of the first eight modes. The dotted area corresponds to stability of the homogeneous equilibrium (5). Crossing each curve from the bottom leads to monotonic loss of local stability of this equilibrium and appearance of waves with wave number k_{mn}. Parameters are $\delta_v = 0.05$, $\delta_p = 0.5$, $P_c = 10$, $L_1 = 1.5$, $L_2 = 1.0$.

$$k_{mn}^2 = \pi^2 \left(\frac{m^2}{L_1^2} + \frac{n^2}{L_2^2} \right). \tag{7}$$

If $\mathrm{Re}\lambda_{mn} > 0$ for at least one pair of integer values m, n, then the perturbations p and $\mathbf{v}$ grow exponentially with time; that is, the homogeneous equilibrium (5) is unstable. Since the first eigenvalue $\lambda_{mn1} = -\delta_v k_{mn}^2$ is negative and does not depend on κ, the stability of the homogeneous distribution is determined only by the roots of the second-degree polynomial $\chi_1(\lambda)$. It is easily seen that if $\kappa = 0$, then all coefficients of $\chi_1(\lambda)$ are positive. This means that in the absence of autotaxis, the equilibrium (5) is always stable; that is, $\mathrm{Re}\lambda_{mn} < 0$ for all m, n (except for $m = n = 0$, corresponding to homogeneous perturbations that we do not consider).

Increasing the value of $\kappa > 0$ can destabilize the equilibrium (5). More precisely, the successive modes (m, n) of the Fourier expansion become excited when the following inequalities are realized:

$$\kappa \overline{P}(P_c - \overline{P}) > \delta_p \delta_v k_{mn}^2 P_c. \tag{8}$$

It can be shown (see app. A in the online edition of the *American Naturalist*) that modes become excited monotonically (i.e., $\mathrm{Im}\lambda_{mn} = 0$).

An obvious necessary condition for instability is $\overline{P} < P_c$; if the average density of animals $\overline{P}$ is greater than the critical density for repulsion P_c, then the spatially homogeneous equilibrium is locally stable for any value of the autotaxis coefficient κ.

The critical stability curves for the first few modes of the homogeneous equilibrium (5) are shown in figure 2 on the parametric plane $(\overline{P}, \kappa)$. For any values of m, n, of the lengths L_1, L_2, and of the nonzero diffusion coefficients δ_p, δ_v, the corresponding mode with wave number k_{mn} can become excited for sufficiently high κ. As shown by inequality (8), the critical values

$$\kappa_{c, mn} = \frac{\delta_p \delta_v k_{mn}^2 P_c}{\overline{P}(P_c - \overline{P})} \tag{9}$$

increase with each diffusion rate δ_p, δ_v. The contrary occurs for the dependence on the domain size: the definition of wave numbers k_{mn} (eq. [7]) shows that the critical values (9) tend to 0 as either side of the rectangle increases.

The linear stability analysis of the one-dimensional case gives the same condition for the monotonic loss of local stability of the homogeneous equilibrium and the emergence of stationary heterogeneous solutions with $k^2 = \pi^2 n^2 / L^2$, where L is the length of the domain and n is the mode number (Senina and Tyutyunov 2002).

The formula (9) for the critical value of the autotaxis coefficient obtained in the case of a rectangular domain can be adapted to the case of a circular domain (as well as app. A, eq. [A9]). Using polar coordinates (r, θ), we performed the linear analysis of model (2)–(4) in a two-dimensional disk of radius ρ. Expanding small initial perturbations of the homogeneous equilibrium $P^*(r, \theta) \equiv \overline{P}, \mathbf{v}^*(r, \theta) \equiv 0$ in a Fourier-Bessel series, we obtained the same instability conditions (8) as in the case of a rectangular domain. In the circular case, the modes are $J_m(k_{mn}r)e^{im\theta}$, where J_m is the Bessel function of the first kind and the wave numbers are defined as $k_{mn} = z_{mn}/\rho$, where z_{mn} is the nth zero of the derivative of J_m.

The polynomial $\chi_1(\lambda)$ (eq. [6b]) obtained in the case of a rectangular domain coincides with the characteristic polynomial common to the cases of one-dimensional and circular domains. This means that the model's response to the increase of the autotaxis coefficient κ is independent of the geometry of the domain. In particular, in all cases considered (two-dimensional rectangle, one-dimensional segment, and circular domain), inequality (8) implies that when the autotaxis coefficient κ increases, modes become excited successively with increasing wave numbers. Thus, the first mode that becomes excited in the case of a rectangular domain is one-dimensional, and the longest side of the rectangle is half of its wavelength. In the case of a disk, the order in which modes k_{mn} become excited corresponds to increasing values of the zeros z_{mn}. The first eight zeros are $z_{11} = 1.8412$, $z_{21} = 3.0542$, $z_{01} = 3.8317$, $z_{31} = 4.2012$ $z_{41} = 5.3175$, $z_{12} = 5.3314$; $z_{51} = 6.4156$, $z_{22} = 6.7061$. The corresponding spatial modes are presented in figure B1 in the online edition of the *American Naturalist*.

Numerical Simulations

The conclusions of the linear analysis, which are valid only locally, must be complemented by numerical simulations of the perturbed dynamics. To study numerically the 1-D and 2-D solutions of model (2)–(4), we discretized the space variables on a grid with 60 nodes in each direction (method of lines). The spatial derivatives were approximated by using second-order central differences in the interior and one-sided differences on the boundary of the domain. The resulting system of ordinary differential equations was integrated with the fourth-order Runge-Kutta method with variable time step. The simulations were also checked with a grid two times as fine. In the 1-D case, the numerical stationary solutions obtained with the method of lines were also obtained with the Galerkin method with 10 modes.

Simulations in both the 1-D and 2-D cases of model (2)–(4) show that, when the parameter κ exceeds the critical value (9), stable clusters are formed. In other words, spatially heterogeneous stationary solutions stabilize. The results presented in this section are a representative selection among the simulations.

One-Dimensional Case

When only one mode is excited, corresponding to the crossing of the first critical curve of the linear stability analysis, a spatially heterogeneous solution emerges, exhibiting a single stationary cluster (see fig. B2*A*). Increasing the autotaxis coefficient κ, the second mode $\kappa = 2$ becomes excited. Starting from a symmetric initial distribution, we obtained different stable symmetric distributions for various values of κ. Three such distributions of the density and the acceleration are shown in figure 3. Further increase of κ results in a more pronounced heterogeneity of the cluster density. Note that the plots of density and acceleration for $\kappa = 0.395$ and $\kappa = 0.5$ are qualitatively similar to the real situation observed for swarming midges (fig. 1). Starting from more heterogeneous symmetric initial distributions and with higher values of κ destabilizing several modes, the 1-D model exhibits high-frequency stationary solutions corresponding to the formation of several clusters (see fig. B2*B*). In more general cases of small initial random perturbation of the unstable homogeneous distributions and with high supercritical values of the autotaxis coefficient κ, we observed rapid formation of regularly spaced transient clusters followed by their subsequent merger into larger groups that finally converged to stationary aggregates either on the right or on the left borders of the domain. From the expressions for λ_{mn} (the roots of the characteristic polynomial [6a] and [6b], given in app. A), it appears that in the case of high κ, when several modes of increasing wave numbers become excited, the faster-growing modes (those with higher λ_{mn}, determining the spatial pattern of the first transient clusters) are modes with intermediate wave numbers.

Two-Dimensional Case

We first consider a square domain with $L_1 = L_2 = 1$. Because the first unstable modes ($m = 1$, $n = 0$ and $m = 0$, $n = 1$) are one-dimensional, the stable heterogeneous solution that occurs for small supercritical $\kappa > \kappa_c$ is one-dimensional (examples of such distributions are shown in fig. 4E, 4F). For higher supercritical κ, and depending on the initial perturbation, true two-dimensional stationary distributions are obtained; starting from different (symmetric or nonsymmetric) initial distributions with an autotaxis coefficient κ corresponding to the wave number $k > \pi(2)^{1/2}$, stabilization of pronounced heterogeneous patterns are observed (fig. 4A–4D).

We then consider a rectangular habitat with unequal sides ($L_1 = 1$, $L_2 = 1.5$). In this case, the two-dimensional heterogeneous stationary solutions that were obtained in the square domain (fig. 4A–4D) can also be realized. However, if the initial perturbation is strong, that is, far from the two-dimensional stationary regime, the solution often evolves to a one-dimensional distribution along the longer side, like those of figure 4E, 4F. This is because the first excited mode is one-dimensional.

Traveling Clusters

The stationary heterogeneous solutions just discussed are in fact the asymptotic states of dynamic solutions that represent the formation of clusters from the initial heterogeneous conditions. Let us consider an example in a square domain with model parameters $\kappa = 3.7$, $\delta_P = 0.5$, $\delta_v = 0.05$, $P_c = 10$, $\overline{P} = 1$, $L_1 = L_2 = 1.5$ (fig. 5). We start with a singular perturbation of the homogeneous equilibrium (fig. 5A). After a short period of dispersal (fig. 5B), animals form an abrupt flat-top cluster with the center at the initial maximum (fig. 5C). Then, this cluster moves to the nearest (right) side of the habitat (fig. 5D, 5E) and thereafter slides slowly to the upper right corner, stabilizing to a stationary heterogeneous distribution (fig. 5F). Transient processes of the same kind, with stabilization of a stationary cluster in the closest corner, were also observed in a rectangular domain, as well as stabilization of one-dimensional nonuniform distributions (fig. 4E, 4F). The observed process presents a traveling pulse-wave dynamic solution, that is, a solitary wave with the density approaching zero both ahead and behind. Such wave solution can obviously be interpreted as the formation and movement of a group of animals.

Starting from initial distributions with multiple peaks, we observed more complex dynamics presenting the formation of several initial clusters, followed by their movement and merger, similar to the transient processes observed in the 1-D case. Note that the stabilized distribution shown in figure 5F is asymmetric because of the asymmetry of the initial distribution. It was also noted above that, although the number of excited modes grows with κ (see condition [8]), the first excited mode is always one-dimensional and has a maximal spatial extension. Because of this, stable heterogeneous regimes are asymmetric in general. The same is true in the one-dimensional case: any symmetric stationary distributions (e.g., figs. 3, B2B) are not stable with respect to small asymmetric perturbations. This result remains valid in the case of a circular domain. The instability of symmetric solutions on a two-dimensional disk is due to the fact that the second subscript of k_{11}, the first mode that becomes excited when κ exceeds its critical value, is odd. This property of the model is demonstrated by the movement of the cluster toward the nearest side of the domain in figure 5. Interestingly, this pattern mimics the so-called wall-following behavior, a phenomenon known in various species, consisting of the "attraction" of animals by the borders and of the tendency to move along them and to form aggregates near the corners (Creed and Miller 1990; Jeanson et al. 2003, 2004).

It is necessary to distinguish the processes that are responsible for forming the cluster and those that maintain its shape during its movement. These two processes strongly interfere in our model because both attraction and repulsion forces are determined at each moment by the cluster profile. In order to study the robustness of our proposed approach and following the scenarios used by Mogilner and Edelstein-Keshet (1999), we made two numerical simulations with two extreme cases of initial distributions: a group with sharp edges (fig. 6A) and an initial profile with a long tail behind the cluster (fig. 6B). For convenience, we only present the one-dimensional version of the model. To relax the influence of domain boundaries, we used a larger domain ($L = 5$).

In the first case, the gradient is initially infinite (or extremely high) at the edges of the rectangular pulse. As shown in figure 6A, after a very short transition period during which diffusion prevails over the directional movement of animals, the cluster restores its shape and starts moving toward the closer boundary, perfectly preserving its shape during the motion as long as it is far from the boundary. This simulation is qualitatively identical to the two-dimensional case presented in figure 5.

The purpose of the second simulation scenario (fig. 6B) was to check the hypothetical possibility of losing the straying individuals that are far behind the moving group. According to the simulation, in a first stage (when the diffusion process is stronger than aggregation), the straying individuals do indeed temporarily form a smaller cluster. However, this secondary group turns out to be absorbed by the main cluster after a short transient during which the clusters are drawn to each other. After completing their

merger, the swarm commences movement toward the right-hand border, approaching the same stationary distribution as in the previous case (shown in fig. 6*A*).

Discussion

Since the behavioral mechanisms that govern the pattern of the clustering phenomenon are still far from being explained in detail and since experimental work is challenging, mathematical modeling provides "a tool for solving the inverse problem, namely, of identifying which of various possible sets of individual interactions might be consistent with the observed pattern of population behavior" (Mogilner and Edelstein-Keshet 1999, p. 537). Furthermore, although there is no doubt that despite many technical difficulties, quantitatively accurate observations of clustering behavior will become available in the next few years (Parrish et al. 2002; Camazine et al. 2003), without mathematical modeling, "these data will not by themselves provide the strong linkage between individual and group characteristics that we require to understand the mechanics and evolution of schooling behavior" (Parrish et al. 2002, p. 297). Making this linkage, models allow investigating "the ability of particular types of behavior algorithms to reproduce observed features of real schools and swarms" guiding "both the modeler and the experimentalist who seek a mean of quantifying aggregation dynamics" (Grünbaum and Okubo 1994, p. 299).

In nature, many mechanisms exist that can lead to the formation of spatial structures. Only one simple mechanism is considered in this article, namely, the ability of animals to aggregate as a result of autotaxis. Although the model incorporates neither individual morphological characteristics nor environmental stimuli nor complex forms of social behavior, our basic phenomenological hypothesis seems to be rather common and plausible, allowing us to explain clustering effects when external factors cannot be considered as aggregating stimuli. It is important to emphasize that the suggested approach for the description of population taxis leads to an extremely simple advection-diffusion system of PDEs. It allows us to obtain spatially heterogeneous regimes while avoiding the complications related to the inclusion of other population dynamic processes acting on a slower timescale.

Compared to our clustering model with autotaxis, classic taxis-diffusion models (e.g., Svirezhev 1987; Murray 1993; Berezovskaya et al. 1999; Petrovskii et al. 2002; Tsyganov et al. 2003) require more complex conditions for the emergence of stable heterogeneous spatial structures. With zero-flux boundary conditions interpreted as a closed habitat, spatially heterogeneous solutions, both stationary and dynamic, arise in such models as a result of the interplay between local kinetics (e.g., recruitment and mortality in a predator-prey system) and spatial dynamics (advection and/or diffusion). Additionally, a necessary condition for the emergence of spatial heterogeneity in these classic models is the presence of at least two interacting species (e.g., a predator and its prey, or a population and an attractive substance; Mimura and Kawasaki 1980; Mimura and Yamaguti 1982; Czárán 1998). Also note that if we assume that the density gradient determines the velocity but not the acceleration, that is, $\mathbf{v} = \kappa\nabla P(1 - P/P_c)$, then the model does not exhibit stable heterogeneous solutions.

The best-known model that describes bacterial aggregation due to tactic movement is the Keller-Segel model of chemotaxis (Keller and Segel 1970). Postulating the proportionality of the chemotactic velocity to the attractant gradient $\mathbf{v} = \kappa\nabla S$, the model includes directional movement but demonstrates unrealistic properties like the possibility of explosion in a finite time if the spatial dimension is >1 (explosion in the one-dimensional case was recently shown not to occur [Osaki and Yagi 2001; Hillen and Potapov 2004]). Hillen and Painter (2001) proposed to modify the Keller-Segel model to prevent overcrowding by assuming that the chemotactic response is reversed to repulsion at high cell densities, that is, $\mathbf{v} = \kappa\nabla S(1 - P/P_c)$ in our notation. This modification allows us to obtain qualitatively adequate solutions describing the process of group formation in population-chemoattractant systems. However, for the autotaxis phenomenon observed for various fish and insect species, the only possible stimulus is the population density itself. Therefore, the approach suggested by Hillen and Painter cannot be used directly in this case.

As already mentioned in the introduction to this article, autotaxis clustering was modeled by Grünbaum (1994) and by Mogilner and Edelstein-Keshet (1999) with an integro-PDE system assuming that the autotaxis velocity is determined by nonlocal information. We have used a different approach. Remaining in the PDE framework, we have built a model in which autotaxis is determined by local information only. Since we postulate that the population density gradient determines the acceleration, the tactic velocity is affected both by the instantaneous gradient and by an inertial component. Earlier, we applied this approach to taxis-diffusion-reaction models of predator-prey systems and showed that it allows spatially heterogeneous regimes in a closed spatial habitat even with no recruitment and mortality in the predator; a patchy distribution of both species is generated by the spatial behavior of the predator only (Arditi et al. 2001; Tyutyunov et al. 2001, 2002).

The inertial (i.e., acceleration) effects of movement, which are neglected in classic chemotaxis models because of the small size of bacteria and hence the high viscosity
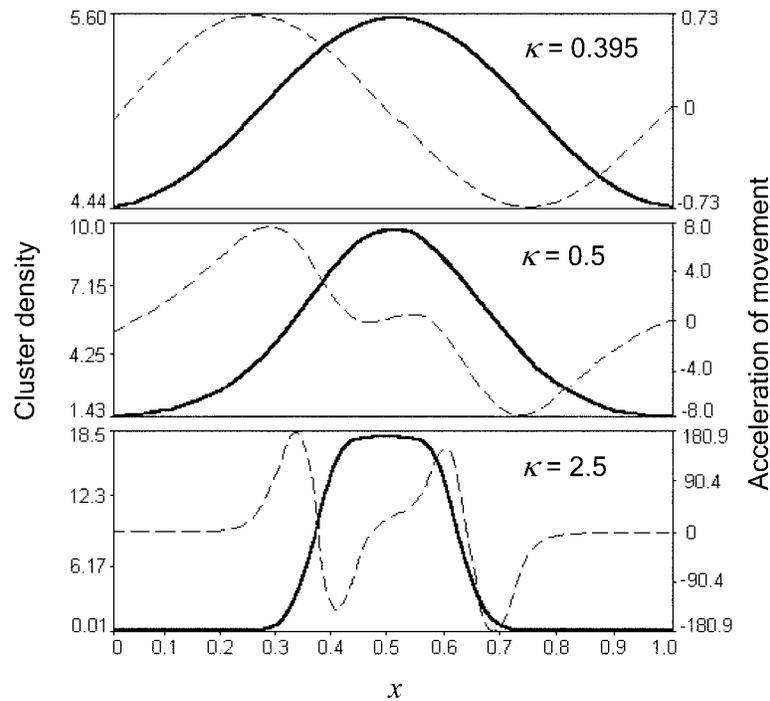
Figure 3: One-dimensional solutions for mode $k = 2$ in the 1-D version of system (2)–(4). Increasing the taxis coefficient κ strengthens the clustering effect. Model parameters are $\delta_v = 0.05$, $\delta_p = 0.5$, $L = 1$, $P_c = 10$, $\overline{P} = 5$. The solid line is the density distribution, and the dashed line is the acceleration.

of the medium, cannot be ignored with insects or fish. In these cases, the hypothesis of equation (3), which is crucial for the appearance of clusters, is well justified. However, the inertial movement of animal density is not necessarily explained by mechanical laws only. Behavioral noninertial responses to the gradient of a decaying chemoattractant emitted by other organisms can lead indirectly to the inertial movement of an individual toward a higher concentration of its conspecifics.

Actually, the link between our autotaxis acceleration approach and the classic chemotaxis model of Keller and Segel (1970) is much stronger than it seems. We show in appendix A that the Keller-Segel model can be written in two equivalent forms: either as a classic system of population-chemo-attractant dynamics or, following our approach, as a system considering the variations of population density and taxis velocity (see app. A for more details). However, as already mentioned, neither of these forms can produce clusters with a realistic profile without a modification preventing overcrowding (Hillen and Painter 2001).

Our system (2)–(4) presents an alternative method that can be used for modeling both autotactic and chemotactic directional movements. The advantage of our approach is clear. With the classic model based on a population-chemoattractant interaction, one needs to deal with the detailed monitoring of the pheromone concentration, which can be an extremely difficult or even impossible task with many natural species. Instead of this, considering only the population density and its velocity, our model is based on a kinematic analysis of animal movement, which is easier to perform following the techniques developed by Okubo and co-workers (see examples in Okubo et al. 1977; Okubo 1980; Parrish and Turchin 1997).

The linear analysis of model (2)–(4) gave us the analytical condition (eq. [8]) for the local instability of the homogeneous equilibrium (5). In particular, we found that with an autotaxis coefficient $\kappa < \kappa_c$, and an average density $\overline{P} < P_c$, the homogeneous stationary solution is locally stable; it loses its stability monotonically when $\kappa > \kappa_c$. For $\overline{P} \geq P_c$, the homogeneous stationary regime is locally stable for any κ. However, numerical simulations have shown that the heterogeneous solutions arising for $\overline{P} < P_c$ can be continued into the parametric domain $\overline{P} \geq P_c$ if the parameter $\overline{P}$ is increased gradually. This means that, for $\overline{P} \geq P_c$, the locally stable homogeneous solution coexists with locally stable stationary heterogeneous regimes.

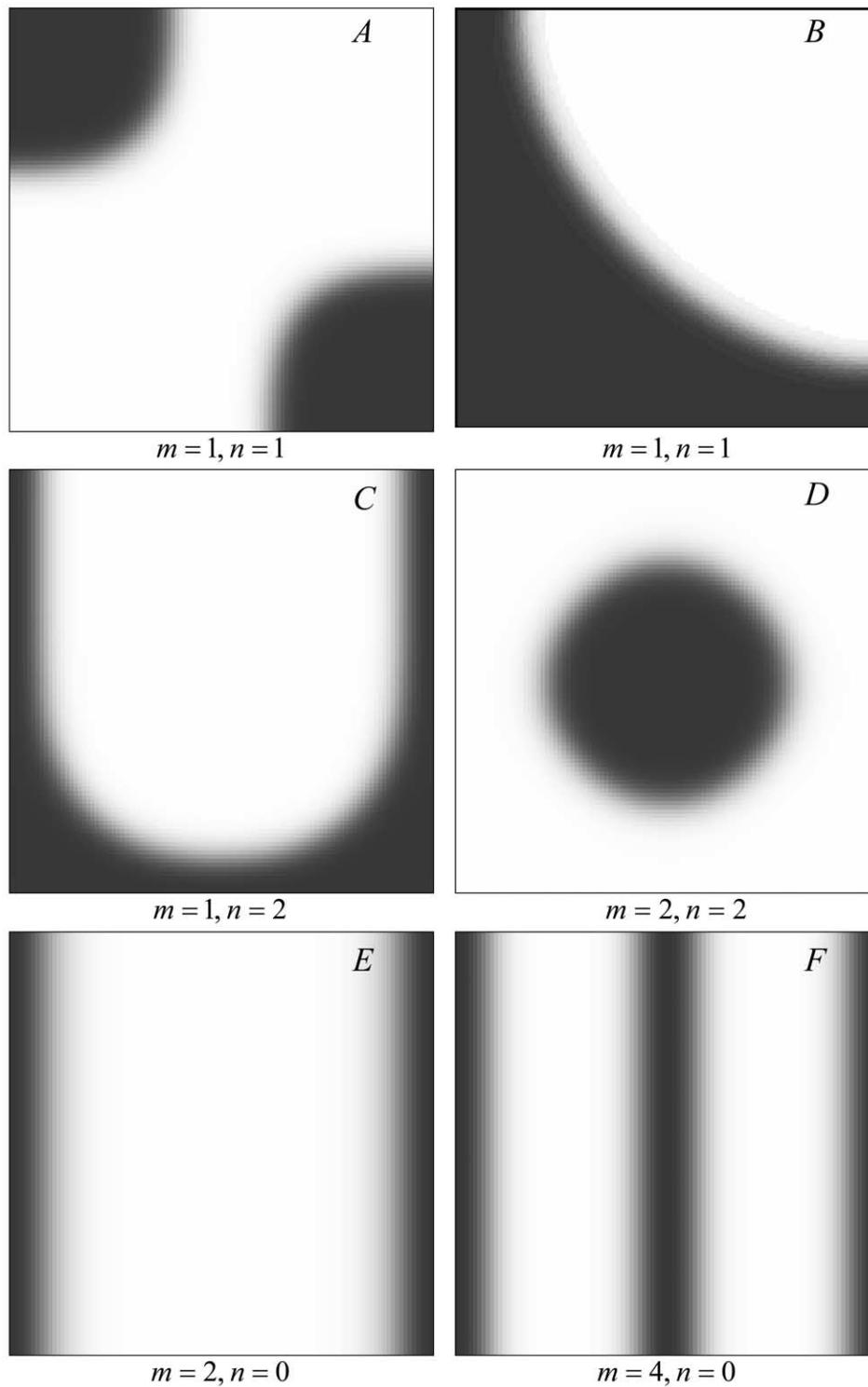Inequality (8) implies that if the population abundance is too high or too low, the homogeneous equilibrium is

Figure 4: Stable spatial structures obtained in the 2-D version of model (2)–(4). The taxis coefficient $\kappa = 3.7$ leads to excitation of several modes. Other parameters are $\delta_v = 0.05$, $\delta_p = 0.5$, $P_c = 10$, $\overline{P} = 5$, $L_1 = L_2 = 1$. Density varies from 0 (*white*) to 20 (*black*).
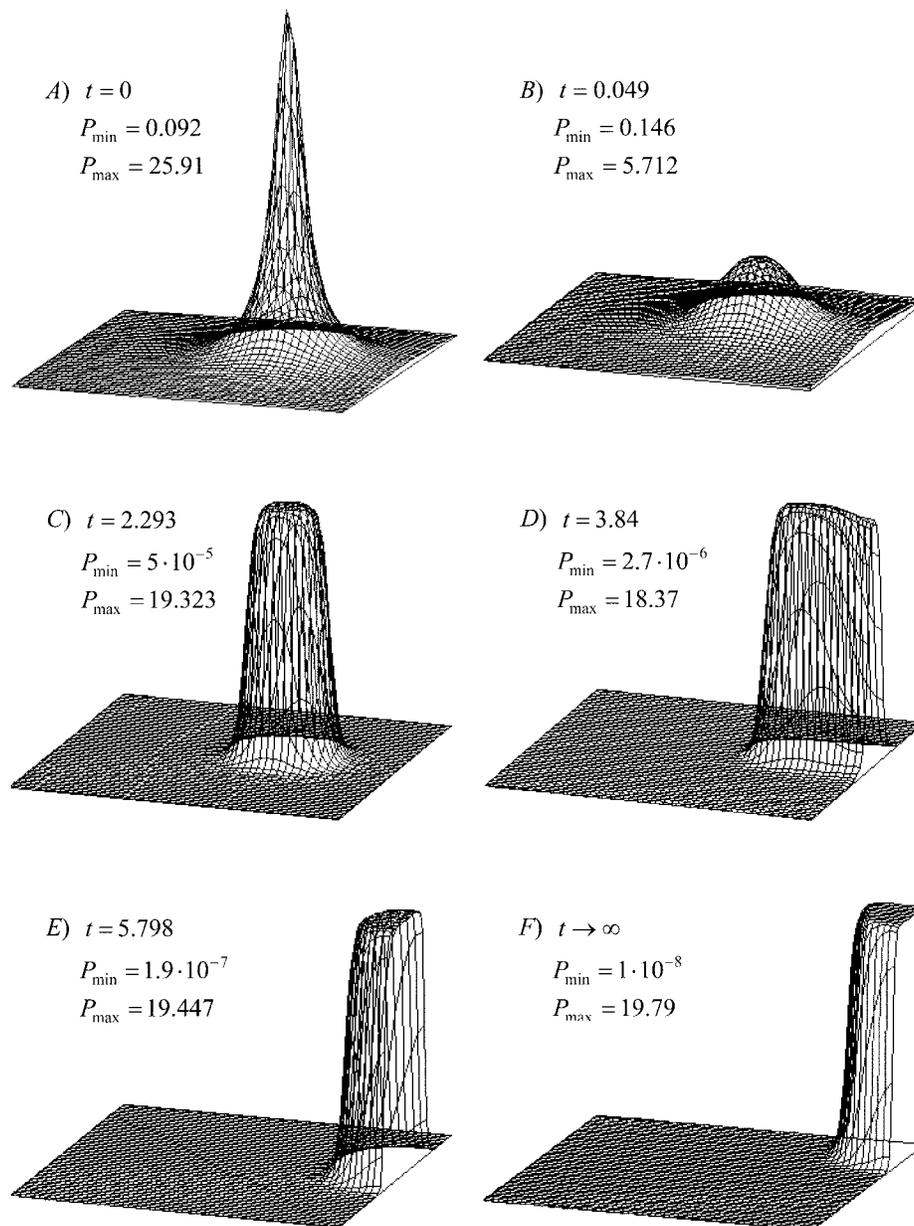
Figure 5: Transient of the population density distribution from the initial singular perturbation to stabilization of the stationary heterogeneous regime.

locally stable. This model property concurs with conclusions based on the integro-PDE swarming model of Grünbaum (1994) and agrees very well with the experimental results of Prigogine and Stengers (1984), Deneubourg et al. (1990), and Camazine et al. (2003), demonstrating a strong relationship between the population density and the level of aggregation. Describing the clustering mechanism of the larvae of a coleopteran (*Dendroctonus micans*)

that aggregates in response to a pheromone gradient, Deneubourg et al. (1990) emphasized that population density determines not only the rate of the aggregation process but also its effectiveness. No stable clusters formed at very low density while at high density, 50% of larvae had clustered within 5 min, and 90% had clustered by 20 min (see also Prigogine and Stengers 1984; Camazine et al. 2003). "At lower densities, the larvae clustered more slowly and
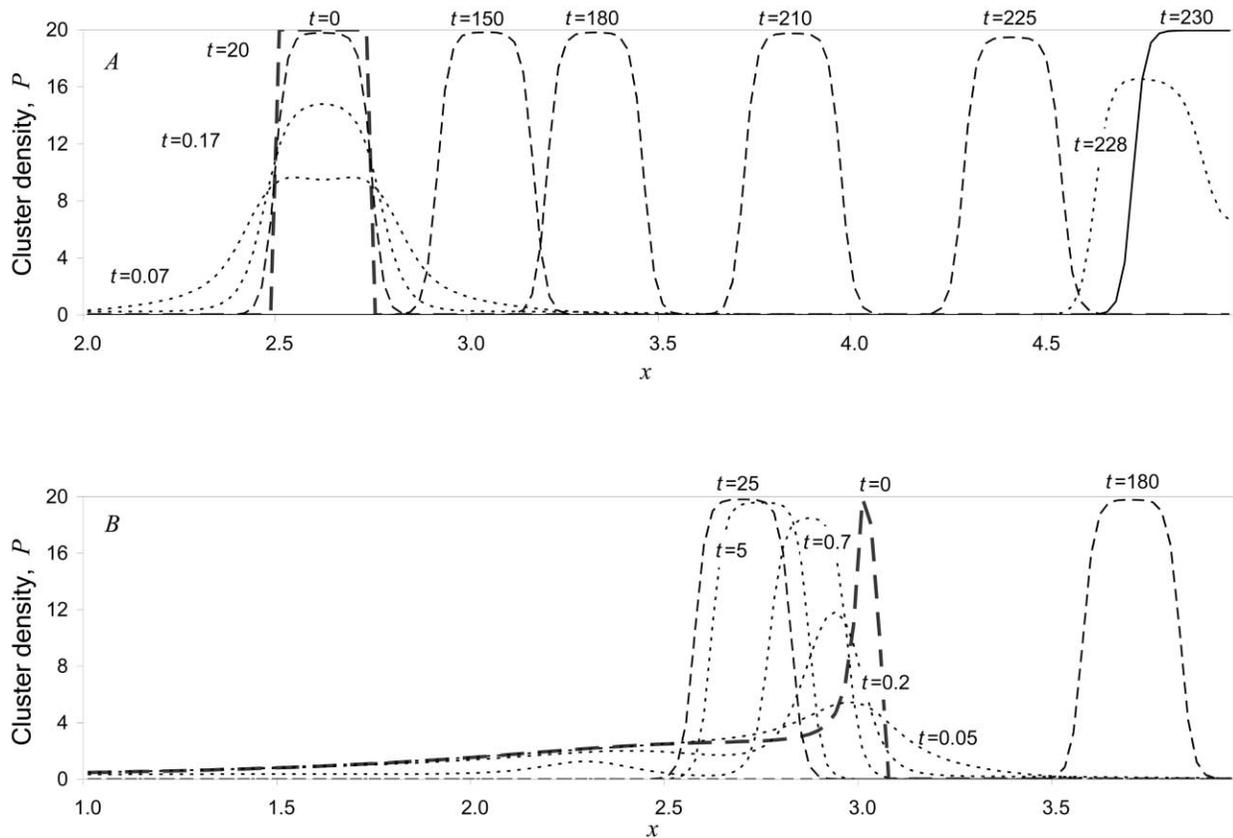
Figure 6: Traveling clusters in the 1-D model, in two extreme cases of initial density distribution. *A*, Rectangular pulse with sharp edges; *B*, diffuse cluster with a long tail. In both cases, the initial profiles (*bold dashed lines*), after a short transient (*thin dotted lines*), stabilize into a cluster (*thin dashed lines*) that moves toward the closer (right-hand) border, perfectly preserving its shape during motion. The final stationary distribution is shown in *A* by the solid line. Model parameters are $\kappa = 4, \delta_v = 0.05, \delta_p = 0.5, L = 5, P_c = 10, \overline{P} = 3$. Note that both graphs show only a portion of the whole domain [0, 5].

the clusters were proportionally smaller" (Camazine et al. 2003, p. 127). Also note that, as it is the case in Grünbaum's (1994) model where all individuals seek some target density (P_c in our notation), the density within the swarm aggregate is substantially higher than the target value (e.g., figs. 3, 5, 6, B2, where $P_c = 10$ in all cases).

Thus, our model (2)–(4) demonstrates the dynamic formation of stationary heterogeneous solutions that have an obvious biological interpretation, self-organization of individuals. These solutions meet the criteria of model adequacy proposed by Mogilner and Edelstein-Keshet (1999): an interior region of approximately uniform distribution, an interface region of sharply decreasing density, and an exterior with a uniformly low number of individuals. Accounting for overcrowding provides a realistic response of the model to an increase of the total population size; simulations show that increasing total population abundance (i.e., increasing $\overline{P}$) does not affect the interior

swarm density but increases the total area occupied by the swarm.

Finally, we have shown that a single autotaxis mechanism based on a plausible assumption about the dependence of animal acceleration on population gradient allows reproducing cluster formation consistent with observations. Since "ideally, both the inputs (i.e., individuals' response to neighbors) and model output (group level characteristics) can be compared to data from real aggregations" (Parrish et al. 2002, p. 298), we hope that the simplicity of the proposed model will stimulate experimentalists to check our central hypothesis and its consequences. The crucial experimental tests should consist of kinematic analyses of animal movement similar to those of Okubo et al. (1977), investigating the relationship between the average acceleration of individuals and the estimated values of density gradient. Both stationary and moving aggregates should be considered in

experimental setups. In particular, the model results about the influence of the domain edges on cluster motion could be compared with observations of species that exhibit wall-following behavior (Jeanson et al. 2004). In order to study the relation of the proposed model to the classic Keller-Segel model, experiments can consider species that exhibit pheromone aggregation like the larvae of the coleopteran (*Dendroctonus micans*) used by Prigogine and Stengers (1984), Deneubourg et al. (1990), and Camazine et al. (2003).

Concluding with remarks about possible applications to natural cases, we note that a similar approach was followed by Seno and Nakai (1995) for modeling shoaling by cichlid fish juveniles (*Lepidiolamprologus elongatus*) in Lake Tanganyika on the basis of experimental data. The authors assumed that two forces affected the movement of each individual in the shoal: an aggregating force (environmental potential) assumed to be directed to the center of the group, and a repulsive force (density-dependent diffusion). The idea of an environmental (or social) potential can also be used in Lagrangian models of swarming (e.g., Gazi and Passino 2003). These models require an explicit determination of the environmental potential (a function that reaches its minimum at the center of the shoal). In contrast, our approach considers an autonomous system and generates clustering even under the assumption that all environmental characteristics are homogeneous and constant; both attraction and repulsion forces are determined by the swarm's profile.

Acknowledgments

Literature Cited

Adioui, M., J.-P. Treuil, and O. Arino. 2003. Alignment in a fish school: a mixed Lagrangian-Eulerian approach. Ecological Modelling 167:19–32.

Arditi, R., Y. Tyutyunov, A. Morgulis, V. Govorukhin, and I. Senina. 2001. Directed movement of predators and the emergence of density-dependence in predator-prey models. Theoretical Population Biology 59:207–221.

Berezovskaya, F. S., A. S. Isaev, G. P. Karev, and R. G. Khlebopros. 1999. The role of taxis in dynamics of forest insects. Doklady Akademii Nauk 365:416–419. [In Russian.]

Breder, C. M., Jr. 1959. Studies on social groupings in fishes. Bulletin of the American Museum of Natural History 117:397–481.

Camazine, S., J.-L. Deneubourg, N. Franks, J. Sneyd, G. Théraulaz, and E. Bonabeau. 2003. Self-organization in biological systems. Princeton University Press, Princeton, N.J.

Cantrell, R. S., and C. Cosner. 2004. Deriving reaction-diffusion models in ecology from interacting particle systems. Journal of Mathematical Biology 48:187–217.

Creed, R. P., Jr., and J. R. Miller. 1990. Interpreting animal wall-following behaviour. Experientia 46:758–761.

Czárán, T. 1998. Spatiotemporal models of population and community dynamics. Chapman & Hall, London.

Deneubourg, J.-L., J.-C. Grégoire, and E. Le Fort. 1990. Kinetics of larval gregarious behavior in the bark beetle *Dendroctonus micans* (Coleoptera: Scolytidae). Journal of Insect Behavior 3:169–182.

Edelstein-Keshet, L., J. Watmough, and D. Grünbaum. 1998. Do travelling band solutions describe cohesive swarms? an investigation for migratory locusts. Journal of Mathematical Biology 36:515–549.

Flierl, G., D. Grünbaum, S. Levin, and D. Olson. 1999. From individuals to aggregations: the interplay between behavior and physics. Journal of Theoretical Biology 196:397–454.

Gazi, V., and K. M. Passino. 2003. Stability analysis of swarms. Institute of Electrical and Electronics Engineers Transactions on Automatic Control 48:692–697.

Govorukhin, V. N., A. B. Morgulis, I. N. Senina, and Y. V. Tyutyunov. 1999. Modelling of active migrations for spatially distributed populations. Surveys of Applied and Industrial Mathematics 6:271–295. [In Russian.]

Govorukhin, V. N., A. B. Morgulis, and Y. V. Tyutyunov. 2000. Slow taxis in a predator-prey model. Doklady Mathematics 61:420–422. [Translated from Doklady Akademii Nauk 372:730–732.]

Grünbaum, D. 1994. Translating stochastic density-dependent individual behavior with sensory constraints to an Eulerian model of animal swarming. Journal of Mathematical Biology 33:139–161.

———. 2002. Predicting availability to consumers of spatially and temporally variable resources. Hydrobiologia 480:175–191.

Grünbaum, D., and A. Okubo. 1994. Modelling social animal aggregations. Pages 296–325 *in* S. Levin, ed. Frontiers in mathematical biology. Springer, New York.

Hillen, T., and K. Painter. 2001. Global existence for a parabolic chemotaxis model with prevention of overcrowding. Advances in Applied Mathematics 26:280–301.

Hillen, T., and A. Potapov. 2004. The one-dimensional chemotaxis model: global existence and asymptotic pro-

file. Mathematical Methods in the Applied Sciences 27: 1783–1801.

Jeanson, R., S. Blanco, R. Fournier, J.-L. Deneubourg, V. Fourcassié, and G. Théraulaz. 2003. A model of animal movements in a bounded space. Journal of Theoretical Biology 225:443–451.

Jeanson, R., C. Rivault, J.-L. Deneubourg, S. Blanco, R. Fournier, C. Jost, and G. Théraulaz. 2004. Self-organized aggregation in cockroaches. Animal Behaviour (in press).

Keller, E. F., and L. A. Segel. 1970. Initiation of slime mold aggregation viewed as an instability. Journal of Theoretical Biology 26:399–415.

Mimura, M., and K. Kawasaki. 1980. Spatial segregation in competitive interaction-diffusion equations. Journal of Mathematical Biology 9:49–64.

Mimura, M., and M. Yamaguti. 1982. Pattern formation in interacting and diffusive systems in population biology. Advances in Biophysics 15:19–65.

Mogilner, A., and L. Edelstein-Keshet. 1999. A non-local model for a swarm. Journal of Mathematical Biology 38:534–570.

Murray, J. D. 1993. Mathematical biology. Springer, Berlin.

Niwa, H.-S. 1996. Mathematical model for the size distribution of fish schools. Computers and Mathematics with Applications 32:79–88.

Okubo, A. 1980. Diffusion and ecological problems: mathematical models. Vol. 10. Biomathematics. Springer, Berlin.

Okubo, A., and S. A. Levin. 2001. Diffusion and ecological problems: modern perspectives. Springer, New York.

Okubo, A., H. C. Chiang, and C. C. Ebbesmeyer. 1977. Acceleration field of individual midges, *Anarete pritchardi* (Diptera: Cecidomyiidae), within a swarm. Canadian Entomologist 109:149–156.

Osaki, K., and A. Yagi. 2001. Finite dimensional attractor for one-dimensional Keller-Segel equations. Funkcialaj Ekvacioj 44:441–469.

Parrish, J. K., and P. Turchin. 1997. Individual decisions, traffic rules, and emergent pattern in schooling fish. Pages 126–142 *in* J. K. Parrish and W. M. Hamner, eds. Animal groups in three dimensions. Cambridge University Press, New York.

Parrish, J. K., S. V. Viscido, and D. Grünbaum. 2002. Self-organized fish schools: an examination of emergent properties. Biological Bulletin 202:296–305.

Petrovskii, S. V., A. Y. Morozov, and E. Venturino. 2002. Allee effect makes possible patchy invasion in a predator-prey system. Ecology Letters 5:345–352.

Prigogine, I., and I. Stengers. 1984. Order out of chaos: man's new dialogue with nature. Bantam, New York.

Sapoukhina, N., Y. Tyutyunov, and R. Arditi. 2003. The role of prey-taxis in biological control: a spatial theoretical model. American Naturalist 162:61–76.

Senina, I. N., and Y. V. Tyutyunov. 2002. Modeling of schooling as a consequence of autotaxis. Zhurnal Obshchei Biologii 63:483–488. [In Russian.]

Seno, H., and K. Nakai. 1995. Mathematical analysis on fish shoaling by a density-dependent diffusion model. Ecological Modelling 79:149–157.

Svirezhev, Y. M. 1987. Nonlinear waves, dissipative structures and catastrophes in ecology. Nauka, Moscow. [In Russian.]

Tsyganov, M. A., J. Brindley, A. V. Holden, and V. N. Biktashev. 2003. Quasisoliton interaction of pursuit-evasion waves in a predator-prey system. Physical Review Letters 91:218102.

Turchin, P. 1998. Quantitative analysis of movement: measuring and modeling population distribution in animals and plants. Sinauer, Sunderland, Mass.

Tyutyunov, Y. V., N. Y. Sapoukhina, A. B. Morgulis, and V. N. Govorukhin. 2001. Mathematical model of active migrations as a foraging strategy in trophic communities. Zhurnal Obshchei Biologii 62:253–262. [In Russian.]

Tyutyunov, Y. V., N. Y. Sapoukhina, I. N. Senina, and R. Arditi. 2002. Explicit model for searching behavior of predator. Zhurnal Obshchei Biologii 63:137–148. [In Russian.]

Appendix A from Y. Tyutyunov et al., "Clustering due to Acceleration in the Response to Population Gradient: A Simple Self-Organization Model"

(Am. Nat., vol. 164, no. 6, p. 722)

Two Alternative Forms of the Keller-Segel Chemotaxis Model

The approach to modeling taxis followed in this study provides a new perspective on the Keller-Segel model. Assuming a zero concentration of the pheromone S on the boundary, one can omit the term $-\nu S$ that describes the decay of the pheromone in the balance equation for S, writing the model of Keller and Segel (1970) in the form

$$\frac{\partial P}{\partial t} + \text{div}(P\nabla S) = \delta_P \Delta P, \tag{A1}$$

$$\frac{\partial S}{\partial t} = \kappa P + \delta_S \Delta S, \tag{A2}$$

$$\mathbf{n} \cdot \nabla P|_{\mathbf{x} \in \partial\Omega} = S|_{\mathbf{x} \in \partial\Omega} = 0. \tag{A3}$$

In model (A1)–(A3) the pheromone concentration S plays the role of a potential function for the taxis velocity; that is, the velocity $\mathbf{v}$ is the gradient of S:

$$\mathbf{v}(\mathbf{x}, t) = \nabla S(\mathbf{x}, t). \tag{A4}$$

Applying the gradient operator to equation (A2) and substituting equation (A4) into model (A1)–(A3), we obtain a model in which the acceleration is proportional to the gradient of the population density P:

$$\frac{\partial P}{\partial t} + \text{div}(P\mathbf{v}) = \delta_{\text{p}} \Delta P, \tag{A5}$$

$$\frac{\partial \mathbf{v}}{\partial t} = \kappa \nabla P + \delta_{\text{v}} \Delta \mathbf{v}, \tag{A6}$$

$$\mathbf{n} \cdot \nabla P|_{\mathbf{x} \in \partial\Omega} = \mathbf{n} \cdot \mathbf{v}|_{\mathbf{x} \in \partial\Omega} = 0, \tag{A7}$$

where $\delta_{\text{v}} = \delta_S$.

Note that the absence of the pheromone decay term $-\nu S$ in equation (A2) is not a crucial simplification. In equation (A6), this term would correspond to "friction" forces, that is, $-\nu \mathbf{v}$. Since this term does not depend on spatial derivatives, it can be considered as a small perturbation of system (A5)–(A7) that cannot cause qualitative changes of its dynamics, at least for small values of ν. Furthermore, taking into account friction forces in our model (2)–(4) modifies only the polynomial χ_1 (eq. [6b]) to

$$\chi_1(\lambda_{mn}) = \lambda_{mn}^2 + [\nu + k_{mn}^2(\delta_{\text{v}} + \delta_{\text{p}})]\lambda_{mn} + \nu\delta_{\text{p}}k_{mn}^2$$
$$+ \delta_{\text{v}}\delta_{\text{p}}k_{mn}^4 - \kappa\overline{P}(1 - \overline{P}/\overline{P_{\text{c}}})k_{mn}^2.$$

The roots of this polynomial are

$$\lambda_{mn2,\,3} \;=\; -\frac{1}{2}\left\{[\nu + (\delta_v + \delta_p)k_{mn}^2] \;\pm\; \sqrt{[\nu + (\delta_v - \delta_p)k_{mn}^2]^2 + 4\kappa\overline{P}(1 - \overline{P}/P_c)k_{mn}^2}\right\}. \tag{A8}$$

Because the discriminant in expression (A8) is always nonnegative, $\lambda_{mn2,\,3}$ are real numbers. Note that the roots of equation (6b) can be obtained from the above expressions by setting $\nu = 0$.

Analyzing the condition for positiveness of the coefficients of the second-degree polynomial $\chi_1(\lambda_{mn})$, it can easily be shown that for any ν, the critical values of the autotaxis coefficient are

$$\kappa_{c,\,mn} \;=\; \delta_p(\delta_v k_{mn}^2 + \nu)\frac{P_c}{\overline{P}(P_c - \overline{P})}. \tag{A9}$$

Comparing this formula with equation (9), one can conclude that increasing friction ν (i.e., the pheromone decay rate) simply increases the bifurcation value κ_c, which will always exist if the necessary condition for instability of the homogeneous distribution, $P_c > \overline{P}$, holds true.

Thus, the Keller-Segel model can be formulated as an autotaxis model with the acceleration proportional to the population density gradient (and a density-dependent coefficient of proportionality preventing overcrowding can provide a qualitatively adequate description of swarming). The reverse is also true, that is, a taxis model built with the acceleration proportional to the gradient of population density $\partial\mathbf{v}/\partial t = \kappa\nabla N$ (e.g., prey-taxis; Arditi et al. 2001) can be rewritten in terms of the classical chemotactic approach with the velocity being the gradient of some potential $S(\mathbf{x}, t)$ that is, $\mathbf{v} = \nabla S$. The potential $S(\mathbf{x}, t)$ does not necessarily represent the concentration of some substance like a pheromone; it can be an abstraction.

Appendix B from Y. Tyutyunov et al., "Clustering due to Acceleration in the Response to Population Gradient: A Simple Self-Organization Model"
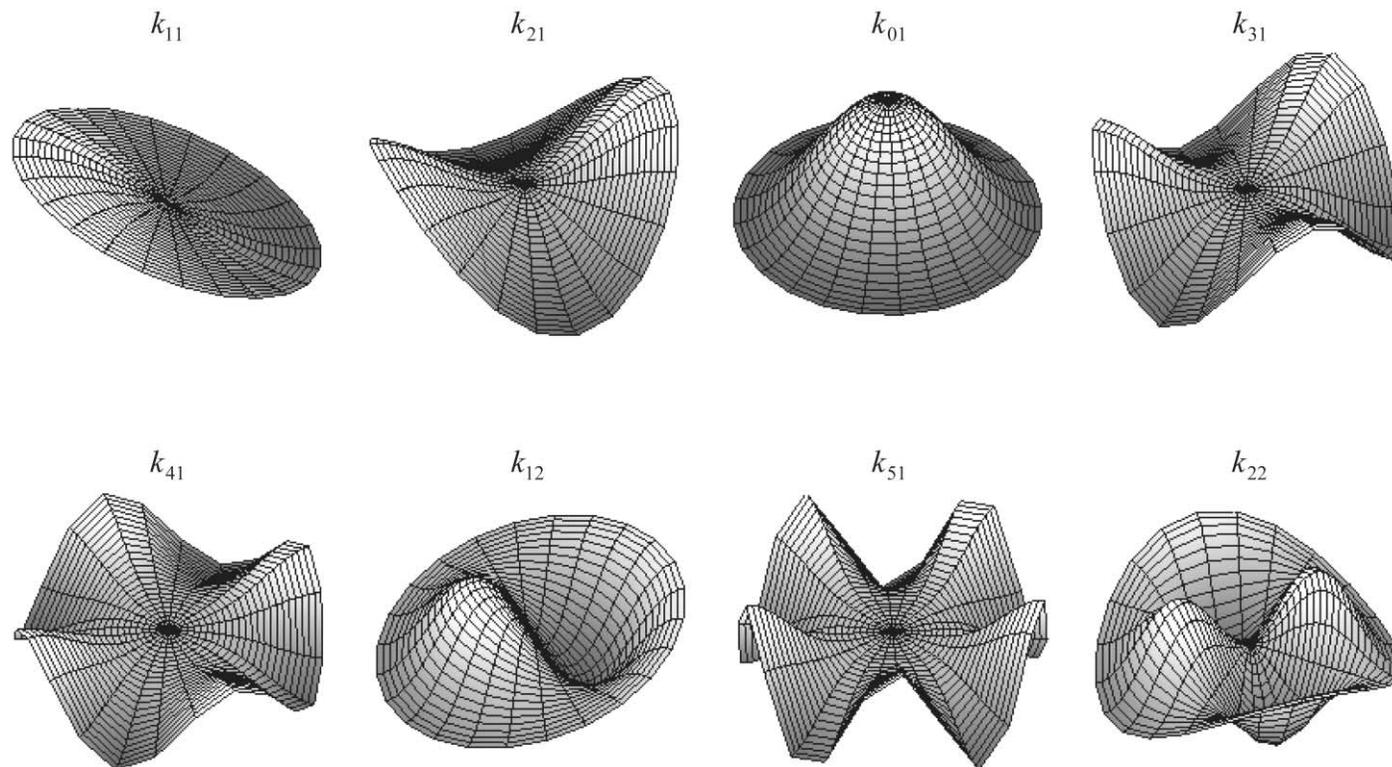
(Am. Nat., vol. 164, no. 6, p. 722)

Figure B1: The first eight Fourier-Bessel modes $J_m(k_{mn}r)e^{im\theta}$ that become excited successively with increasing autotaxis coefficient κ in the case of a circular domain. These functions are the analogues of the simple Fourier functions of the 1-D and rectangular 2-D domains. Note that, as in these cases, the first excited mode k_{11} has the widest extension.
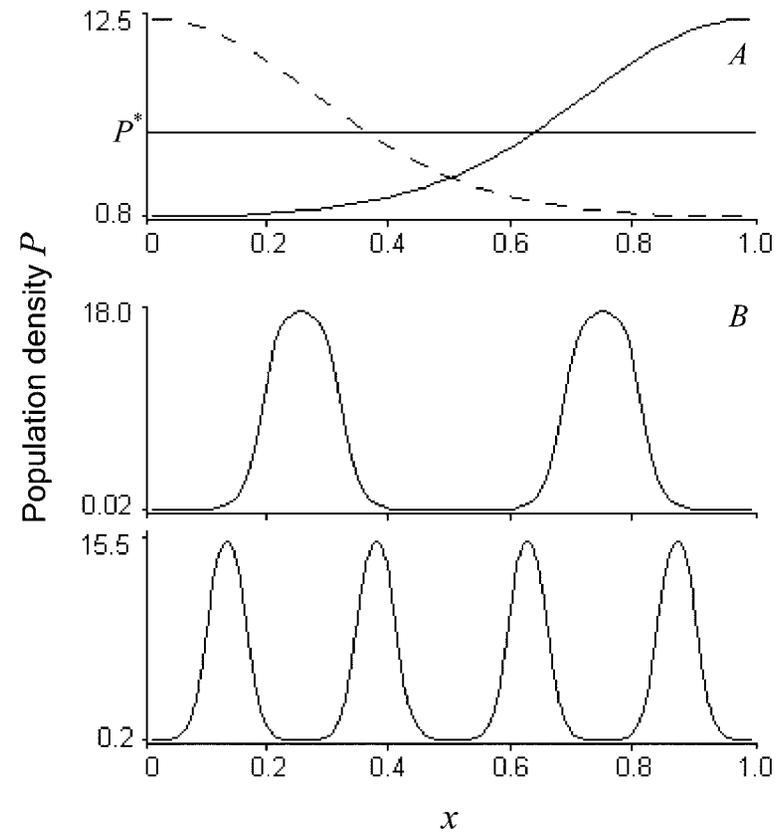
Figure B2: One-dimensional nonuniform stable stationary distributions. *A*, Solutions that can be obtained both in the 1-D and 2-D formulations of model (2)–(4). In fact, two symmetric solutions (with aggregates either on the left or on the right bounds) arise simultaneously, each being realized depending on the initial spatial distribution; $\kappa = 1.5$, mode $k = 1$ is excited. *B*, High-frequency stable distributions that can emerge from spatial perturbations with initial central symmetry; upper graph: $\kappa = 7.0$, mode $k = 4$ is excited; lower graph: $\kappa = 15.0$, mode $k = 8$ is excited.